Statistics of shadowing time in nonhyperbolic chaotic systems with unstable dimension variability

Younghae Do[1] and Ying-Cheng Lai[1,2]

[1]*Department of Mathematics and Statistics, Arizona State University, Tempe, Arizona 85287, USA*
[2]*Departments of Electrical Engineering and Physics, Arizona State University, Tempe, Arizona 85287, USA*
(Received 17 July 2003; published 30 January 2004)

Severe obstruction to shadowing of computer-generated trajectories can occur in nonhyperbolic chaotic systems with unstable dimension variability. That is, when the dimension of the unstable eigenspace changes along a trajectory in the invariant set, no true trajectory of reasonable length can be found to exist near any numerically generated trajectory. An important quantity characterizing the shadowability of numerical trajectories is the shadowing time, which measures for how long a trajectory remains valid. This time depends sensitively on initial condition. Here we show that the probability distribution of the shadowing time contains two distinct scaling behaviors: an algebraic scaling for short times and an exponential scaling for long times. The exponential behavior depends on system details but the small-time algebraic behavior appears to be universal. We describe the computational procedure for computing the shadowing time and give a physical analysis for the observed scaling behaviors.

I. INTRODUCTION

The validity of numerical computations is a fundamental problem in chaotic dynamical systems because of their sensitive dependence on initial conditions. Given a chaotic system, one can compute a numerical trajectory, starting from a random initial condition, and ask whether there is a true trajectory of the system dynamics, starting from a slightly different initial condition [1] that stays in a small neighborhood of the numerical one. This is the problem of *shadowing of numerical trajectories*. From a different standpoint, one can also ask, by computing an ensemble of numerical trajectories, whether the statistical (ergodic) averages computed using these trajectories are approximations of the true ones of the system. This is the problem of *shadowing of statistical averages* [2,3]. Depending on the specifics of the problem that one is dealing with, either the former or the latter problems, or both, can be important. This paper concerns the fundamental dynamical process involved in the first problem.

Existing results on shadowing of numerical trajectories build upon the important mathematical notion of hyperbolicity. Roughly speaking, the dynamics is hyperbolic on a chaotic set if, at each point of the trajectory, the tangent space is split into expanding and contracting subspaces and the angles between them are bounded away from zero. Furthermore, the expanding subspace at each point evolves into the expanding one along the trajectory and the same is true for the contracting subspace. Otherwise the set is nonhyperbolic. The following results have been established regarding shadowing: (1) hyperbolic chaotic systems permit shadowing of numerical trajectories for an infinitely long time [4]; (2) for nonhyperbolic chaotic systems in which the splitting into the expanding and contracting subspaces is continuous but there are tangencies at which the two subspaces coincide, shadowing can be expected for a finite amount of time that depends on the computer roundoff error [5,6]; and (3) if a continuous splitting of the subspaces is not possible, i.e., if the dimensions of the expanding and contracting subspaces are not constant on different parts of the invariant set (called *un-*

stable dimension variability), then shadowing of numerical trajectories for appreciable lengths of time becomes unlikely [7–10].

A key quantity to characterize shadowing dynamics is the *shadowing time τ*, which measures for how long a numerical trajectory remains valid in the sense that it stays close to a true trajectory. For a given trajectory, this time can be computed by monitoring the evolution of the *pointwise shadowing distance*, the local phase-space distance between a given numerical trajectory and a true trajectory. For hyperbolic systems, the shadowing time is infinite for numerical trajectories from random initial conditions [4]. For nonhyperbolic systems with tangencies, the average shadowing time is inversely proportional to the square root of the computer roundoff [5]. Nonhyperbolicity caused by unstable dimension variability, common in high-dimensional chaotic systems with multiple positive Lyapunov exponents, has begun to be understood [7–10]. Current results [7–9] indicate that, for such a system, the shadowing distance typically increases exponentially after encountering a glitch point where a change in the unstable dimension occurs, then decreases exponentially in hyperbolic regions, and so on, with a lower bound determined by the computer roundoff. The switches between the expanding and contracting behaviors occur randomly in time, suggesting that the behavior of the logarithm Z of the pointwise shadowing distance mimics that of a random walker. A calculation of the corresponding first-passage time gives the average shadowing time, which depends on the system details in the following manner:

$$\langle \tau \rangle \sim \delta^{-2m/\sigma^2}, \tag{1}$$

where δ is the computer roundoff, and $m>0$ and σ are the mean and standard deviation of the time-one Lyapunov exponent that is closest to zero [11].

The aim of this paper is to report our findings concerning the shadowing dynamics for nonhyperbolic systems with unstable dimension variability. We focus on the shadowing time τ. Due to chaos, this time depends sensitively on initial con-

69 016213-1

ditions and thus can be regarded as a random variable for trajectories from different random initial conditions. Our principal result, which concerns the probability distribution $\Phi(\tau)$ of the shadowing time, is that $\Phi(\tau)$ contains both universal and nonuniversal scaling features. For small τ values the distribution exhibits a universal algebraic scaling while the distribution is exponential for large values of τ. The exponential distribution depends on system details. In particular, we have

$$\Phi(\tau) \sim \begin{cases} \tau^{-3/2} & \text{for small } \tau \\ \exp(-a\tau) & \text{for large } \tau, \end{cases} \qquad (2)$$

where the constant a is system dependent. The scaling law means that for nonhyperbolic systems with unstable-dimension variability, shadowing of numerical trajectories can be expected only in short time because longer shadowing times are exponentially improbable. A brief account of this work has appeared recently [12].

We shall present numerical results to support the scaling law (2) and a physical analysis to explain it. The analysis is based on the similarity between the dynamics of shadowing and that of a random walk, briefly described as follows. When a trajectory moves on the attractor, it encounters both hyperbolic region, where it converges to a true trajectory, and nonhyperbolic region with unstable dimension variability in which the numbers of local stable and unstable directions change. Thus, in hyperbolic region, Z "walks" randomly toward the reflecting barrier because, in this case, shadowing theory guarantees the existence of a nearby true trajectory [4]. Insofar as the trajectory is in a hyperbolic region, on average, the pointwise shadowing distance can be adjusted in such a way that it decreases exponentially in time toward the lower bound δ. When a nonhyperbolic region with unstable dimension variability is encountered, the sudden change of an expanding direction into a contracting one, or conversely, immediately destroys the consistency of the adjustment process, and the pointwise shadowing distance tends to increase exponentially. In the Z space, there is an excursion away from the reflecting barrier. The Fokker-Planck equation, which describes the evolution of the probability distribution of the walker's motion, in combination with the proper initial and boundary conditions, can be solved to yield the scaling law (2).

In Sec. II, we review the basic concepts essential for understanding the shadowing dynamics. In Sec. III, we detail a procedure to compute the shadowing distance and the shadowing time. In Sec. IV, we present numerical results with two examples: a three-dimensional map that we have constructed to specifically address the dynamics of shadowing in high-dimensional chaotic systems, and the kicked double-rotor map [13] that has been a prototype model for addressing the issues of unstable dimension variability and shadowing [7,9,14]. In Sec. V, we present a physical theory to explain the numerical observed scaling behavior of the shadowing time. A brief discussion is presented in Sec. VI.

II. BASIC CONCEPTS IN SHADOWING DYNAMICS

A. Shadowing in hyperbolic systems

The dynamics on an invariant set is hyperbolic if, at each point of the trajectory, the tangent space can be split into expanding and contracting subspaces and the angle between them is bounded away from zero. Furthermore, the expanding subspace evolves into the expanding one along the trajectory and the same holds for the contracting subspace.

The existence of a true trajectory near any numerical trajectory in hyperbolic systems can be understood by noting that, along the stable direction, the distance between the true and numerical trajectories decreases exponentially in forward time, while along the unstable direction, the distance decreases exponentially in backward time. Given a numerical trajectory, a true trajectory can be found to stay in the neighborhood of the numerical one. Specifically, consider the set of phase-space vectors that represent the difference between the true and numerical trajectories. Then, the stable component of the vector can be constructed by following the dynamics in the stable direction starting from the initial condition, which decreases exponentially in forward time, while the unstable component can be located by following the unstable dynamics starting from the end point of the numerical trajectory, which contracts exponentially in backward time. Combining the stable and unstable components of the difference vectors along the numerical trajectory yields a true trajectory that stays within δ [4]. All these can be done because of the hyperbolic structure of the dynamics.

The shadowing lemma of Anosov and Bowen [4], which holds for hyperbolic systems, can be extended to nonuniformly hyperbolic systems [17].

B. Shadowing in nonhyperbolic systems with tangencies

Shadowing of numerical trajectories in nonhyperbolic systems, for which tangencies are the sole source of nonhyperbolicity, is reasonably well understood [5,6]. Near a tangency, the dynamics is neither expanding nor contracting, much like what happens near a critical point of a one-dimensional map where the derivative is zero. Tangencies encountered in low-dimensional chaotic systems are typically quadratic. The breakdown of shadowing can thus be intuitively demonstrated by considering the logistic map: $x_{n+1} = 4x_n(1-x_n)$. A numerical trajectory can be kicked out of the unit interval $[0,1]$ and iterates to $x = -\infty$ if it comes within about $\sqrt{\delta}$ of the critical point $x = 1/2$. For an ergodic trajectory, the probability density function is smooth near the critical point. The probability for the breakdown of shadowing is thus proportional to $\sqrt{\delta}$, which means that the time required for this to happen is proportional to $\delta^{-1/2}$. Thus, if the computer roundoff is $\delta \sim 10^{-16}$, the length of the numerical trajectory for which shadowing is guaranteed is about 10^8 iterations. For a continuous-time flow, this means that numerical trajectories containing less than 10^8 passings of a Poincaré surface of section, or about 10^8 oscillations, are reliable. Such a time can be considered sufficient for many practical computations.

C. Unstable dimension variability and breakdown of shadowing

The breakdown of shadowing in the presence of unstable dimension variability was first pointed out by Abraham and Smale [15], who constructed a simple ergodic invariant set in $\mathcal{R}^D$ with two saddle fixed points, A and B, which have one and two local unstable directions, respectively. Trajectories in the invariant set can spend arbitrarily long times near each point. Imagine a ball of initial conditions starting near A, which has a $(D-1)$-dimensional stable subspace. As the map is iterated, the ball of initial conditions is stretched into a thin curve along $W^u(A)$. The corresponding numerical trajectories lie within δ of this thin curve. Consider a phase space of $D=3$ dimensions. In the plane spanned by the two stable directions at A, all computer-generated trajectories lie in a circle of radius δ centered at A. That both fixed points are embedded in the same ergodic invariant set means that some time later, trajectories near A visit a neighborhood of B. When this happens, the trajectories begin to separate along the new unstable direction. Along this direction, numerical and true trajectories separate from each other exponentially with time at a rate determined by the eigenvalue associated with the fixed point B. The numerical trajectories no longer shadow the true trajectories at B. The switching from A to B is called a *glitch*.

A characteristic feature of a chaotic invariant set is that an infinite number of unstable periodic orbits are embedded in it. If the chaotic set has unstable dimension variability, typically the infinite set of periodic orbits consists of subsets with distinct unstable dimensions. Each subset has an infinite number of orbits that are dense on the invariant set. Thus, there are infinitely many glitches. In general, numerical trajectories cannot be shadowed by any true trajectory for long.

III. PROCEDURE TO COMPUTE THE SHADOWING DISTANCE AND TIME

A. Pointwise shadowing distance and brittleness

For nonhyperbolic invariant set Λ, a way to quantify the violation of continuous shadowing is to examine the pointwise shadowing distance. Let $\{\mathbf{p}_n\}_{n=0}^N$ denote a numerical trajectory, or a *pseudo-trajectory*, of length $N+1$. Because of the computer roundoff, typically there is a small difference between $\mathbf{p}_{n+1}$ and $\mathbf{f}(\mathbf{p}_n)$ for $n=0,1,\ldots,N-1$, where $\mathbf{f}(\mathbf{p}_n)$ is the image of the point $\mathbf{p}_n$ under the true dynamics. Let δ be an upper bound for all these errors along the pseudotrajectory, i.e., $|\mathbf{p}_{n+1}-\mathbf{f}(\mathbf{p}_n)|<\delta$, for $n=0,\ldots,N-1$. A true trajectory $\{\mathbf{x}_n\}_{n=0}^N$, on the other hand, satisfies $\mathbf{f}(\mathbf{x}_n)=\mathbf{x}_{n+1}$, for $n=0,\ldots,N-1$. The true trajectory ϵ *shadows* the pseudotrajectory if $|\mathbf{x}_n-\mathbf{p}_n|<\epsilon$ for $n=0,\ldots,N$. The quantity $|\mathbf{x}_n-\mathbf{p}_n|$ is the *pointwise* or *local* shadowing distance [7,9]. The *brittleness* $\mathcal{B}$ of a pseudotrajectory $\{\mathbf{p}_n\}_{n=0}^N$ is the ratio of the shadowing distance over the magnitude of the one-step error,

$$\mathcal{B} \equiv \frac{(\text{shadowing distance})}{(\text{one-step error})} = \frac{\max_n|\mathbf{p}_n-\mathbf{x}_n|}{\delta}. \qquad (3)$$

For hyperbolic systems, the pointwise shadowing distance is on the order of δ because every pseudotrajectory is shadowable, and $\mathcal{B}$ is of order 1. For nonhyperbolic systems, however, the pointwise shadowing distance can reach the size of the entire attractor, and $\mathcal{B}$ can be on the order of the inverse of the computer roundoff error.

B. Test brittleness

The brittleness $\mathcal{B}$ generally is not computable, as the true trajectory is unknown. The *test brittleness* is a first-order approximation to the brittleness, which can be computed without a precise knowledge of the true trajectory. Given a pseudotrajectory $\{\mathbf{p}_n\}_{n=0}^N$, the refinement procedure [5] detailed below can be used to find an approximately true trajectory, say $\{\mathbf{y}_n\}_{n=0}^N$. The test brittleness B is defined as $B \equiv \max_n|\mathbf{p}_n-\mathbf{y}_n|/\delta$. The idea of the refinement method is to correct the pseudotrajectory at each point in a proper way so that the resulting trajectory is closer to a true trajectory (or less noisy). Let $\mathbf{c}_n$ be the correction vector such that $\mathbf{y}_n=\mathbf{p}_n+\mathbf{c}_n$. For the corrected trajectory $\{\mathbf{y}_n\}_{n=0}^N$ to be as close as possible to a true trajectory, we require $\mathbf{f}(\mathbf{y}_n)=\mathbf{y}_{n+1}=\mathbf{p}_{n+1}+\mathbf{c}_{n+1}$. Assuming that the correction vector is small, a first-order approximation yields

$$\mathbf{p}_{n+1}+\mathbf{c}_{n+1}=\mathbf{f}(\mathbf{p}_n+\mathbf{c}_n)\approx\mathbf{f}(\mathbf{p}_n)+\mathbf{D}\cdot\mathbf{f}(\mathbf{p}_n)\cdot\mathbf{c}_n, \qquad (4)$$

where $\mathbf{D}\cdot\mathbf{f}(\mathbf{p}_n)$ is the Jacobian matrix of partial derivatives evaluated at $\mathbf{p}_n$. Let $\mathbf{e}_n=\mathbf{p}_n-\mathbf{f}(\mathbf{p}_{n-1})$ be the error at the nth step of the iteration. Then $\mathbf{f}(\mathbf{p}_n)=\mathbf{p}_{n+1}+\mathbf{e}_{n+1}$, which, when substituting in Eq. (4), yields

$$\mathbf{c}_{n+1}\approx\mathbf{D}\cdot\mathbf{f}(\mathbf{p}_n)\cdot\mathbf{c}_n+\mathbf{e}_{n+1} \quad \text{for} \quad n=0,\ldots,N-1. \qquad (5)$$

This iteration scheme is unstable because $\mathbf{D}\cdot\mathbf{f}$ has unstable eigenspaces at each point. Instead, we decompose the tangent space of the Jacobian matrix $\mathbf{D}\cdot\mathbf{f}(\mathbf{p}_n)$ into stable and unstable subspaces. In the stable subspace, forward iterations yield the stable component of $\mathbf{c}_n$, while in the unstable subspace, backward iterations yield the unstable component of $\mathbf{c}_n$. For a given pseudotrajectory of length $(N+1)$, the combination of the results from the forward and backward iterations then yields the required correction vector $\mathbf{c}_n$. These correction vectors are used to approximate the corresponding pointwise shadowing distances.

The refined trajectory $\{\mathbf{y}_n\}_{n=0}^N$ to be computed contains $(N+1)D$ unknowns, while Eq. (5) contains only ND equations. Thus, to guarantee a unique solution, D boundary conditions must be specified for the refinement process. If there are D_S and D_U stable and unstable directions, respectively, along the pseudotrajectory, then we choose $\mathbf{c}_N$ to be in the D_S-dimensional stable subspace at $\mathbf{p}_N$ and $\mathbf{c}_0$ to be in the D_U-dimensional unstable subspace at $\mathbf{p}_0$, which together give D additional D boundary conditions [5]. These boundary conditions guarantee that outside the time interval $[0,N]$, the correction vector $\mathbf{c}$ decreases to 0 exponentially, so that the refined trajectory converges to the true one. In particular, since $\mathbf{c}_N$ is in the stable subspace of $\mathbf{p}_N$, it converges to $\mathbf{0}$ under the forward map for time beyond N, and likewise, since $\mathbf{c}_0$ is in the unstable subspace at $\mathbf{p}_0$, it will approach

asymptotically to **0**, too, under the inverse map for time steps preceding 0. Let $\mathbf{c}_n = \mathbf{s}_n + \mathbf{u}_n$, where $\mathbf{s}_n$ and $\mathbf{u}_n$ are the stable and unstable components of $\mathbf{c}_n$, respectively. The boundary conditions are $\mathbf{s}_0 = \mathbf{0}$ and $\mathbf{u}_N = \mathbf{0}$. Under these Eq. (5) yields the following set of iterative schemes for solving the stable and unstable components of the perturbation vector along the entire pseudotrajectory:

$$\mathbf{s}_{n+1} = \mathcal{S}_p[\mathbf{D} \cdot \mathbf{f}(\mathbf{p}_n) \cdot \mathbf{s}_n + \boldsymbol{\delta}_n],$$

$$\mathbf{u}_n = \mathcal{U}_p[\mathbf{D} \cdot \mathbf{f}^{-1}(\mathbf{p}_{n+1}) \cdot (\mathbf{u}_{n+1} - \boldsymbol{\delta}_{n+1})], \tag{6}$$

for $n = 0, \ldots, N-1$, where $\mathcal{S}_p$ and $\mathcal{U}_p$ are the projection operators into the stable and unstable subspaces, respectively, which can be determined by the spans of the stable and unstable subspaces at every point of the pseudotrajectory. The computation of the stable and unstable subspaces can be carried out straightforwardly [16] by using the standard Gram-Schmidt orthonormalization procedure contained in, for instance, the algorithm for computing the Lyapunov spectrum [18]. After all the correction vectors are computed, the test brittleness is obtained: $B = \max_n |\mathbf{c}_n| / |\mathbf{e}_n|$.

The refinement procedure relies on a continuous decomposition of the tangent space along the pseudotrajectory. The set of computed correction vectors (equivalently, the estimated pointwise shadowing distances) are bounded by the size of the chaotic invariant set in the phase space. As a result, the magnitude of the test brittleness should be of the order of the inverse of the computer roundoff. If there is unstable dimension variability, the stable and unstable projection matrices can be extremely ill conditioned, resulting in extraordinarily large correction vectors. Despite this difficulty, we can take the viewpoint that very large values of the test brittleness suggest breakdowns of shadowing at various points of the pseudotrajectory and, the refinement scheme provides a numerical way to find glitches on the chaotic set.

IV. NUMERICAL EXAMPLES

A. A three-dimensional map

We have constructed a three-dimensional map for which, in a convenient parameter range, there is a transition to high-dimensional chaotic attractors with two positive Lyapunov exponents and consequently severe unstable dimension variability near the transition. The map reads

$$x_{n+1} = \cos(\alpha x_n + 0.6\alpha y_n),$$

$$y_{n+1} = 0.6\alpha z_n \cos(y_n - z_n),$$

$$z_{n+1} = 0.1\alpha x_n \sin(1 - z_n), \tag{7}$$

where α is the bifurcation parameter. Figures 1(a) and 1(b) show a bifurcation diagram and the Lyapunov spectrum versus α, respectively. In the parameter range considered, there is at least one positive Lyapunov exponent (except for periodic windows). Transition to high-dimensional chaos occurs at $\alpha = \alpha_c \approx 6.0$, where the second largest Lyapunov exponent becomes positive. We thus expect severe unstable dimension variability and consequently breakdown of shadowing to oc-
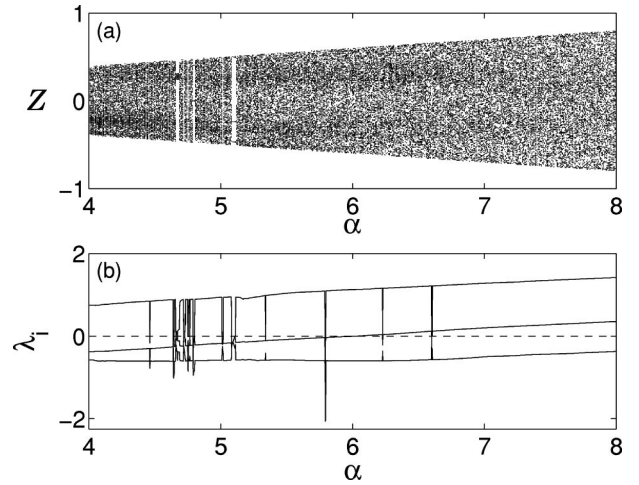

FIG. 1. For the three-dimensional map Eq. (7), (a) a bifurcation diagram, and (b) a Lyapunov bifurcation diagram. We see that bifurcation to high-dimensional chaos with two positive Lyapunov exponents occurs at $\alpha = \alpha_c \approx 6.0$. Severe unstable dimension variability and the consequent breakdown of shadowing can be expected for α near α_c.

cur [19] for α near the critical value α_c. The portraits of typical low- and high-dimensional chaotic attractors are shown in Figs. 2(a) and 2(b) for $\alpha = 4.0$ and $\alpha = 8.0$, respectively. The low-dimensional chaotic attractor appears to have some visible structures of unstable foliations, while the high-dimensional chaotic attractor looks apparently more "random" and space filling.

Figures 3(a)–3(c) show the evolution of the pointwise shadowing distance for three different parameters. We see
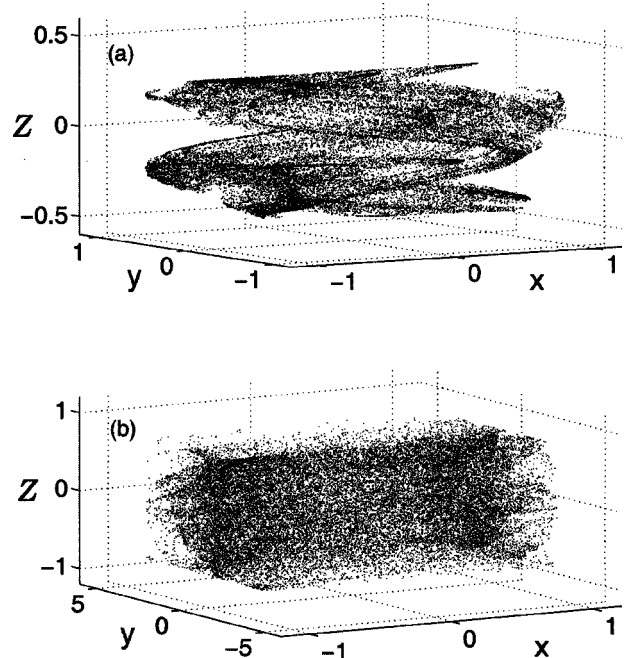

FIG. 2. For the three-dimensional map Eq. (7), portraits of (a) a low-dimensional chaotic attractor with one positive Lyapunov exponent for $\alpha = 4.0$, and (b) a high-dimensional attractor with two positive exponents for $\alpha = 8.0$.
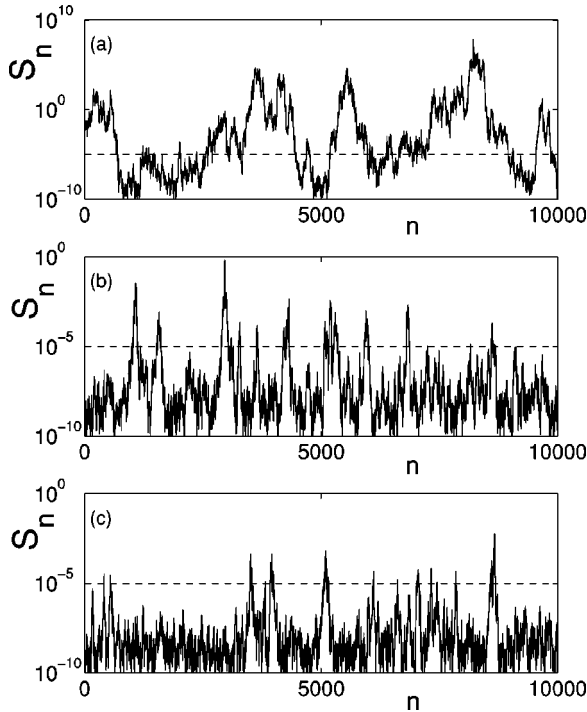
FIG. 3. For the three-dimensional map Eq. (7), the pointwise shadowing distance $\mathbf{s}_n$ computed from a trajectory of length 10^4 for (a) $\alpha=6.0$, (b) $\alpha=6.2$, and (c) $\alpha=6.4$. The dashed line corresponds the threshold $\epsilon=10^{-5}$.

that the distances can be large for $\alpha=6.0$ (a). For $\alpha=6.2$ (b) and $\alpha=6.4$ (c), the distances are relatively smaller, as unstable dimension variability is relatively less severe because the second largest Lyapunov exponent is not as close to zero as in the case of $\alpha=6.0$. The shadowing time can be conveniently computed as the time interval during which the pointwise shadowing distance stays less than $\epsilon\ll 1$. With the seemingly random variations in the pointwise shadowing distance, the shadowing time can be regarded as a random variable. To obtain the probability distributions of the shadowing time, we construct histograms of the values of time intervals τ during which the shadowing distance is less than the threshold $\epsilon=10^{-5}$. Figure 4(a) shows, on logarithmic scale, the probability distributions of shadowing time for $\alpha=6.0$, $\alpha=6.2$, and $\alpha=6.4$. We see that, for small τ values the distributions tend to collapse onto a single line of slope $-3/2$, indicating a universal algebraic scaling. For large values of τ, the distributions are apparently exponential, as can be seen in the corresponding plots on a semilogarithmic scale in Fig. 4(b). We have observed numerically similar behaviors for other values of α near α_c.

B. The kicked double-rotor map

We consider a physical system, the kicked double rotor, which has been a paradigmatic model for addressing high-dimensional chaotic phenomena [13], particularly the shadowing problem [7]. The kicked double-rotor map describes the time evolution of an idealized mechanical system consisting of two thin, massless rods as shown in Fig. 5. The
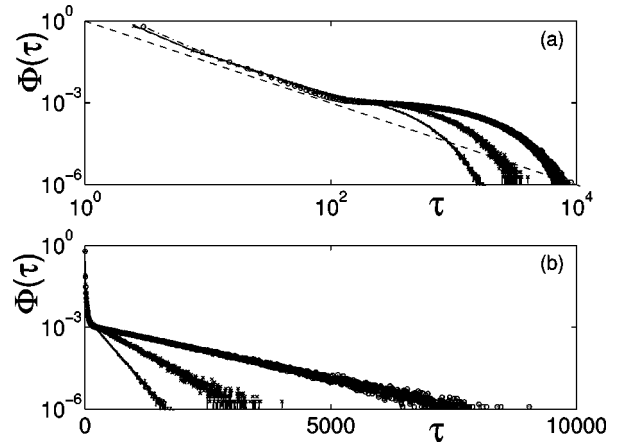

FIG. 4. (a), (b) For the three-dimensional map Eq. (7), probability distributions of the shadowing time τ for $\alpha=6.0$ (thin solid line), $\alpha=6.2$ (crosses + dashed line), and $\alpha=6.4$ (circles + thin solid line). In (a), the distributions are shown on a logarithmic scale, indicating a universal algebraic scaling behavior with exponent $-3/2$ for small values of τ. In (b), the distributions are plotted on a semilogarithmic scale, revealing an exponential decaying behavior that depends on the system details.

first rod, of length l_1, rotates about the fixed pivot P_1. The second rod, of length $2l_2$, pivots about P_2, which moves. A mass m_1 is attached at P_2, and two masses $m_2/2$ are attached to each end of the second rod. The end of the second rod (P_3) receives vertical periodic impulse kicks of period T and amplitude ρ. The rotors move in the horizontal plane so that gravity can be neglected. Friction at the pivots P_1 and P_2 is proportional to the angular velocity $d\theta_1(t)/dt$ and $d\theta_2(t)/dt-d\theta_1(t)/dt$ with proportionality constants ν_1 and ν_2, respectively. Due to the periodic forcing, the set of differential equations describing the double rotor can be reduced to the following four-dimensional map by using the stroboscopic sectioning technique [13]:

$$\begin{pmatrix} \mathbf{X}_{n+1} \\ \mathbf{Y}_{n+1} \end{pmatrix} = \begin{pmatrix} \mathbf{M}\cdot\mathbf{Y_n}+\mathbf{X_n} \\ \mathbf{L}\cdot\mathbf{Y_n}+\mathbf{G}(\mathbf{X_{n+1}}) \end{pmatrix}, \tag{8}$$

where $\mathbf{X}=(x^1,x^2)^T$, $\mathbf{Y}=(y^1,y^2)^T$, x^1 and x^2 are the angular
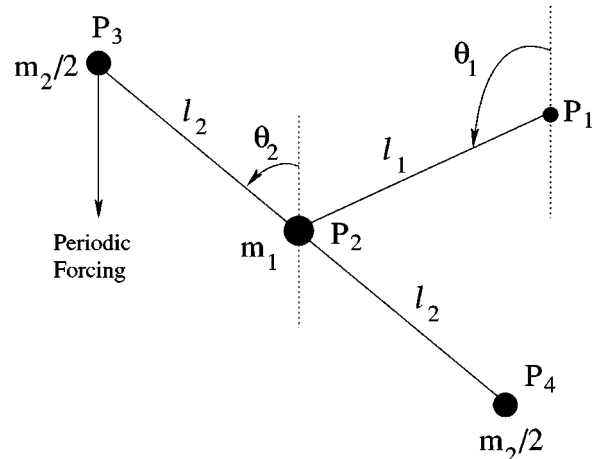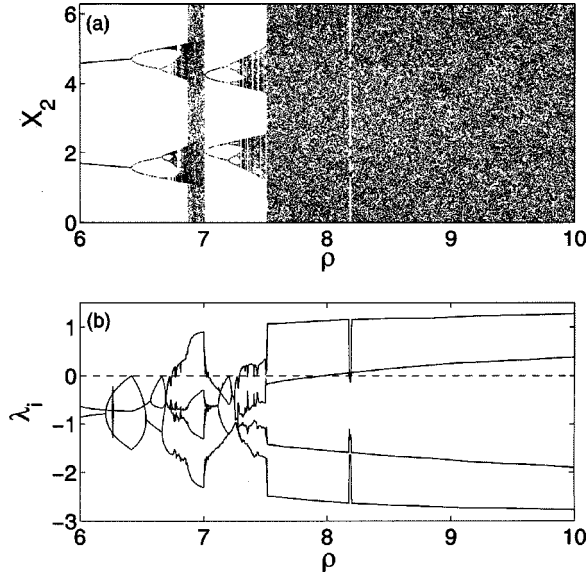

FIG. 5. The kicked double-rotor system.

FIG. 6. (a) Bifurcation diagram and (b) Lyapunov exponent vs the kicking parameter ρ for the double-rotor map Eq. (8). Transition to low-dimensional chaos with one positive Lyapunov exponent, through a cascade of period-doubling bifurcations, occurs at $\rho \approx 6.7$. Bifurcation to high-dimensional chaos with two positive Lyapunov exponents occurs at $\rho \approx 8.0$, at which there is severe unstable dimension variability.

positions of the rods at the instant of the nth kick, and y^1 and y^2 are the angular velocities of the rods immediately after the nth kick. $\mathbf{L}$ and $\mathbf{M}$ are constant 2×2 matrices defined by

$$\mathbf{L} = \sum_{j=1}^{2} \mathbf{W}_j e^{\lambda_j T}, \quad \mathbf{M} = \sum_{j=1}^{2} \mathbf{W}_j \frac{e^{\lambda_j T} - 1}{\lambda_j}, \quad (9)$$

where

$$\mathbf{W}_1 = \begin{pmatrix} a & b \\ b & d \end{pmatrix}, \quad \mathbf{W}_2 = \begin{pmatrix} d & -b \\ -b & a \end{pmatrix},$$

$$a = \frac{1}{2}\left(1 + \frac{\nu_1}{\Delta}\right), \quad d = \frac{1}{2}\left(1 - \frac{\nu_1}{\Delta}\right), \quad b = -\frac{\nu_2}{\Delta},$$

$$\lambda_{1,2} = -\frac{1}{2}(\nu_1 + \nu_2 \pm \Delta), \quad \Delta = \sqrt{\nu_1^2 + 4\nu_2^2}. \quad (10)$$

The function $\mathbf{G}(\mathbf{X})$ is given by

$$\mathbf{G}(\mathbf{X}) = \begin{pmatrix} c_1 \sin x^1 \\ c_2 \sin x^2 \end{pmatrix}, \quad (11)$$

where $c_1 = \rho l_1 / I$, $c_2 = \rho l_2 / I$, and $I = (m_1 + m_2) l_1^2 = m_2 l_2^2$. For illustrative purposes we fix $\nu = T = I = m_1 = m_2 = l_2 = 1$ and $l_2 = 1/\sqrt{2}$. These parameters yield

$$\mathbf{L} = \begin{pmatrix} 0.241\,427\,724 & 0.272\,608\,938 \\ 0.272\,608\,938 & 0.514\,036\,662 \end{pmatrix},$$
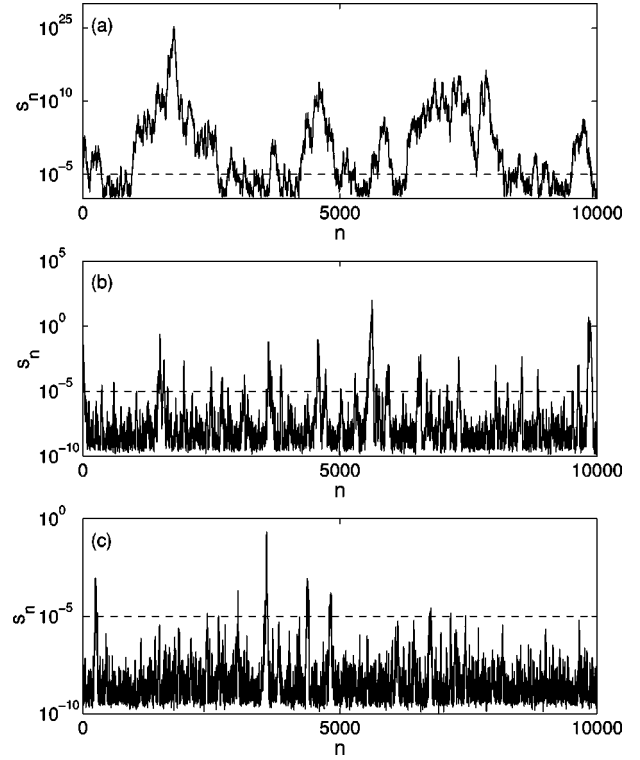

FIG. 7. For the double-rotor map Eq. (8), the pointwise shadowing distance s_n computed from a trajectory of length 10^4 for (a) $\rho = 8.0$, (b) $\rho = 8.5$, and (c) $\rho = 9.0$. The dashed line corresponds to the threshold $\epsilon = 10^{-5}$.

$$\mathbf{M} = \begin{pmatrix} 0.485\,963\,338 & 0.213\,354\,401 \\ 0.213\,354\,401 & 0.699\,317\,739 \end{pmatrix}.$$

We choose the kicking strength ρ as the bifurcation parameter. A typical bifurcation diagram is shown in Fig. 6(a), and the Lyapunov spectrum of the attractor versus ρ is shown in Fig. 6(b). As ρ is increased, a cascade of period-doubling bifurcations occurs, which leads to low-dimensional chaotic attractors with one positive Lyapunov exponent at $\rho \approx 6.7$. A large periodic window occurs for $7.0 \lesssim \rho \lesssim 7.5$. At $\rho \approx 8.0$, the second largest Lyapunov exponent becomes positive, leading to high-dimensional chaotic attractors with two positive exponents for $\rho \gtrsim 8.0$. We thus expect severe unstable dimension variability and breakdown of shadowing for $\rho \approx 8.0$ [7,14,19]. As ρ is increased from 8.0, unstable dimension variability becomes less severe.

Figures 7(a)–7(c) show the pointwise shadowing distance s_n as a function of n, computed from a trajectory of length 10^4 on the chaotic attractor for $\rho = 8.0$, $\rho = 8.5$, and $\rho = 9.0$, respectively. Because of the severe unstable dimension variability for $\rho = 8.0$, numerical trajectories cannot be shadowed for appreciable lengths of time. This situation is reflected in the variations of the pointwise shadowing distance over many orders of magnitude. The huge values of the pointwise shadowing distance arise from ill conditioning of the refinement technique, due to the sudden and frequent changes in the dimensions of the stable and unstable subspaces along the trajectory. In contrast, for $\rho = 8.5$ and $\rho = 9.0$, there are time intervals in which the pointwise shad-
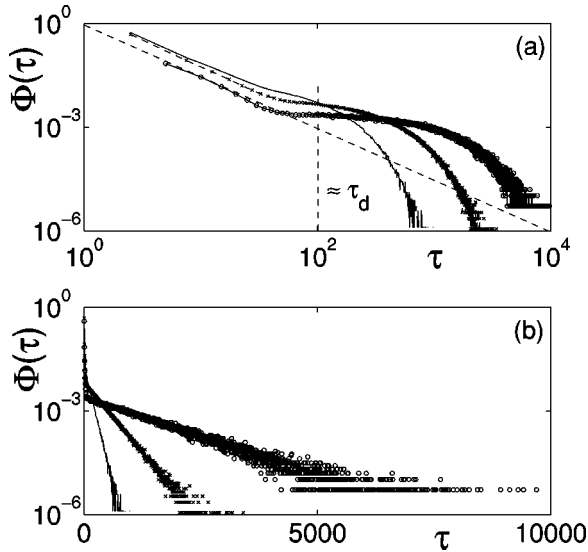
FIG. 8. (a), (b) For the double-rotor map Eq. (8), probability distributions of the shadowing time τ for $\rho \equiv \rho_0 = 8.0$ (thin solid line), $\rho = 8.5$ (crosses + dashed line), and $\rho = 9.0$ (circles + thin solid line). In (a), the distributions are shown on a logarithmic scale, indicating a universal algebraic scaling behavior with exponent $-3/2$ for small values of τ. In (b), the distributions are plotted on a semilogarithmic scale, indicating an exponential decaying behavior.

owing distances are much less than 1, and the fluctuations in the distances are much smaller than those for $\rho = 8.0$, indicating less severe obstructions to shadowing [7]. As shown in Fig. 6(b), for $\rho = 8.5$ and $\rho = 9.0$, the second largest Lyapunov exponent lies away from 0 and, in fact, the distributions of its finite-time approximations have much smaller variance [7].

Figure 8(a) shows, on a logarithmic scale, for $\epsilon = 10^{-5}$, the histograms of shadowing time for $\rho = 8.0$ (thin solid line), $\rho = 8.5$ (crosses + dashed line), and $\rho = 9.0$ (circles + thin solid line), respectively. We observe that for $\tau < \tau_d$ $\approx 10^2$, the distributions $\Phi(\tau)$ appear to be algebraic, while for $\tau > \tau_d$, $\Phi(\tau)$'s decrease rapidly with τ. The decaying behavior of $\Phi(\tau)$ for $\tau > \tau_d$ appears to be exponential, as shown on a semilogarithmic scale in Fig. 8(b). The exponential decay is system dependent in the sense that its rate depends on the parameter ρ. In particular, the rate is large for $\rho = 8.0$, indicating that it is highly improbable to have a long shadowing time, due to the severe unstable dimension variability at this parameter value. As ρ is increased from 8.0, the degree of unstable dimension variability is reduced so that the exponential decay in $\Phi(\tau)$ becomes slower. Again, the remarkable feature is that the algebraic decay for small τ appears to be *universal* with the scaling exponent $-3/2$, which holds for many other values of ρ in the interval [7,8,10] that we have examined.

V. PHYSICAL THEORY FOR STATISTICS OF SHADOWING TIME

To explain the universal and nonuniversal features in shadowing, as exemplified by Figs. 4 and 8, we consider a random walk model. To refresh, a trajectory encounters both approximately hyperbolic regions and regions with glitches. The shadowing dynamics in the hyperbolic regions are equivalent to a random walk toward the reflecting barrier corresponding to the computer roundoff. As we have described, an approximation of the true trajectory can be found with a refinement technique that adjusts the points on the trajectory in a consistent manner along the stable and unstable directions. As a result, insofar as the trajectory is in a hyperbolic region, on average, the pointwise shadowing distance decreases exponentially with time toward the lower bound δ. When a glitch occurs, the consistency in the trajectory adjustments, which can be achieved in hyperbolic regions, is immediately destroyed, causing the pointwise shadowing distance to increase in an exponential manner. In the walker's space, it is equivalent to an excursion away from the reflecting barrier.

We are thus led to consider the following model:

$$s_{n+1} = w_n s_n, \tag{12}$$

where s_n stands for the shadowing distance at time n, and w_n is a random variable that describes the expansion or contraction of the local shadowing distance at time n. Introducing a new variable $y_n = \log_{10} s_n$, we obtain

$$y_{n+1} = y_n + \nu + z_n, \tag{13}$$

where $\nu \equiv \langle \log_{10} w_n \rangle$ is the drift of the random walk and $z_n = \log_{10} w_n - \langle \log_{10} w_n \rangle$ is a zero mean random variable. Approximately [20], we can write down the Fokker-Planck equation

$$\frac{\partial P}{\partial t} = -\nu \frac{\partial P}{\partial y} + \frac{D}{2} \frac{\partial^2 P}{\partial y^2}, \tag{14}$$

where $P(t, y)$ is the probability distribution for observing the walker at distance y at time t, and the diffusion coefficient is given by $D = \langle z_n^2 \rangle$. For computing the probability distribution of the shadowing time, the maximum relevant pointwise shadowing distance is $y_{th} = \log_{10} \epsilon$, the threshold distance below which shadowing is considered to hold. There is thus an absorbing boundary condition at y_{th},

$$P(t, y_{th}) = 0. \tag{15}$$

The shadowing distance cannot be smaller than the computer roundoff δ, which stipulates a reflecting boundary condition at $\log_{10} \delta$:

$$\left[J(t, y) \equiv -\nu P + \frac{D}{2} \frac{dP}{dy} \right]\bigg|_{y = \log_{10} \delta} = 0. \tag{16}$$

Assuming the walker starts at an arbitrary place $\log_{10} \delta < y_0 < y_{th}$ at $t = 0$, we have the initial condition

$$P(0, y) = \delta(y - y_0). \tag{17}$$

Under these boundary and initial conditions, the Fokker-Planck equation can be solved [21], which gives the follow-
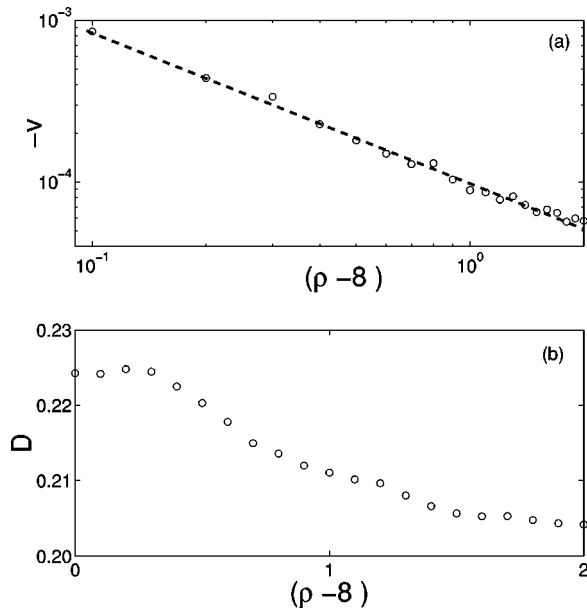
FIG. 9. For the double-rotor map Eq. (8), (a) draft v and (b) diffusion D coefficients.

ing probability distribution for the first-passage time of the walk across y_{th} (the shadowing time):

$$\Phi(\tau) \sim \frac{\tau^{-3/2}}{\sqrt{2\pi D}} \exp\left(-\frac{\nu^2 \tau}{2D}\right), \qquad (18)$$

where the proportional constant depends on the choice of the initial condition y_0. For small values of τ, the dependence of $\Phi(\tau)$ on τ is mainly algebraic with the universal scaling exponent of $-3/2$. For large values of τ, the exponentially decaying behavior in $\Phi(\tau)$ dominates with the rate given by $a = \nu^2/(2D)$. These are the scaling results in Eq. (2). The dependence of the exponential rate on system details can be assessed by computing the dependence of the diffusion parameters ν and D on a system parameter. We find that, approximately, the average drift depends inversely on the parameter variation: $|\nu| \sim 1/(\rho - \rho_0)$, for $\rho > \rho_0 \approx 8.0$, and the diffusion coefficient D is relatively constant, as shown in Fig. 9.

A few remarks are in order.

(1) The average drift ν, which is a key parameter in the random-walk model, decreases as ρ is increased from ρ_0. In fact, the value of the average drift appears to be maximum when unstable dimension variability is most severe. This is expected from Figs. 7(a)–7(c), the plots of the logarithmic pointwise shadowing distance, or the displacement of the random walker for different values of ρ, where we see that the apparently random evolution of the distance indeed exhibits much larger drift for $\rho = \rho_0$, compared with other values of ρ. Dynamically, this happens due to the existence of the maximally possible number of glitches on the attractor for $\rho = \rho_0$ when unstable dimension variability is most severe. As a result, the pointwise shadowing distance suffers a relatively large number of expanding phases as compared with the number of contracting phases experienced in the

hyperbolic regions, leading to an appreciable amount of drift in the random walk model. This is somewhat different from the diffusion model used in Ref. [9].

(2) The solution to the Fokker-Planck equation, under the boundary and initial conditions, gives satisfactory explanations for our numerical results. The setting of the initial and boundary value problem is in fact quite standard [21], and it also appears in other contexts such as noisy on-off intermittency [23,24]. Our results are completely consistent with those in that context.

(3) Between the universal scaling in $\Phi(\tau)$ (algebraic) and the nonuniversal scaling (exponential) regimes, there is a crossover regime in τ where both the algebraic and exponential contributions are important. This is the so-called "shoulder regime" in noisy on-off intermittency [23]. The crossover time is approximately given by $\tau_d \approx D^{-1}[\ln(\epsilon/\delta)]^2$, which defines the time scale of diffusion [24]. There is another time of interest, which is the drift time $|\nu|^{-1} \ln(\epsilon/\delta)$. These represent the typical times for the shadowing distance to reach the threshold from the level of computer roundoff due to diffusion and drift, respectively.

VI. DISCUSSION

In summary, we have uncovered universal and nonuniversal features in the shadowing dynamics of nonhyperbolic chaotic systems with unstable dimension variability [22]. Our results provide a fairly detailed understanding of the fundamental problem of shadowing in terms of statistical characterizations. Our theoretical explanation suggests that the shadowing problem shares the same dynamical mechanism as that for on-off intermittency under noise.

The problem of shadowing is closely related to a more fundamental question: is mathematical modeling a meaningful approach for high-dimensional chaotic systems with unstable dimension variability? The relation between shadowing and modeling can be stated more precisely [25]. Generally, a necessary requirement for a model is robustness under small perturbations. One can generate outputs from two versions of the model using slightly different parameter values or initial conditions. Chaotic processes depend sensitively on both. A model is considered robust if the sets of all possible outcomes of two slightly different versions of the model are similar. Difficulties arise when trajectories from one version of the model are not shadowable by trajectories from another, as occurs in the presence of unstable dimension variability. In such cases, the model may be useless for making detailed predictions about the behavior of particular initial conditions, although statistical predictions may still be possible [14]. The results of this paper shed light on for how long one can expect solutions from a model to be approximately valid [26].

[1] Because of the sensitivity of a chaotic system to initial conditions and parameters, the existence of the computer roundoff error means that two trajectories starting from exactly the same initial condition will diverge exponentially from each other in time. Shadowing of a trajectory by another one is possible only when they start from slightly different initial conditions.

[2] The first paper, to our knowledge, addressing shadowing of statistical averages is T. Sauer, Phys. Rev. E **65**, 036220 (2002), which deals with nonhyperbolic chaotic systems with unstable dimension variability.

[3] A common situation where statistical averages depend on noise is when the system is in a periodic window, where a periodic attractor and a nonattracting chaotic invariant set (chaotic saddle) coexist in the phase space, For small noise, a trajectory can remain in the neighborhood of the periodic attractor indefinitely. As the noise amplitude exceeds a critical value, the trajectory on the periodic attractor can be perturbed away from it to visit the chaotic saddle. As the saddle is nonattracting, the trajectory will go back to the original periodic attractor, be kicked away again, and so on. Noise thus induces an intermittent behavior. It has been shown recently that statistical averages associated with the intermittency scale with the noise amplitude algebraically [Y.-C. Lai, Z. Liu. G. Wei, and C.-H. Lai, Phys. Rev. Lett. **89**, 184101 (2002)].

[4] D.V. Anosov, Proc. Steklov Inst. Math. **90**, 1 (1967); R. Bowen, J. Diff. Eqns. **18**, 333 (1975).

[5] S.M. Hammel, J.A. Yorke, and C. Grebogi, J. Complex. **3**, 136 (1987); Bull. Am. Math. Soc. **19**, 465 (1988); C. Grebogi, S.M. Hammel, J.A. Yorke, and T. Sauer, Phys. Rev. Lett. **65**, 1527 (1990); T. Sauer and J.A. Yorke, Nonlinearity **4**, 961 (1991).

[6] S.N. Chow and K.J. Palmer, J. Dyn. Differ. Equ. **3**, 361 (1991); S.N. Chow and E.S. Van Vleck, SIAM J. Sci. Comput. (USA) **15**, 959 (1994).

[7] S.P. Dawson, C. Grebogi, T. Sauer, and J.A. Yorke, Phys. Rev. Lett. **73**, 1927 (1994).

[8] S.P. Dawson, Phys. Rev. Lett. **76**, 4348 (1996); E.J. Kostelich, I. Kan, C. Grebogi, E. Ott, and J.A. Yorke, Physica D **109**, 81 (1997); E. Barreto and P. So, Phys. Rev. Lett. **85**, 2490 (2000).

[9] T. Sauer, C. Grebogi, and J.A. Yorke, Phys. Rev. Lett. **79**, 59 (1997).

[10] Y.-C. Lai and C. Grebogi, Phys. Rev. Lett. **82**, 4803 (1999); Y.-C. Lai, D. Lerner, K. Williams, and C. Grebogi, Phys. Rev. E **60**, 5445 (1999).

[11] While Lyapunov exponents are asymptotic quantities defined with respect to the natural measure of the chaotic attractor, the relevant entities that determine the shadowing dynamics are the statistical characteristics of the distribution of the finite-time Lyapunov exponents. Say one chooses an ensemble of random initial conditions, computes the exponents in a finite time, and then constructs histograms of these exponents. The mean values of the histograms are the asymptotic exponents.

[12] Y. Do, Y.-C. Lai, Z. Liu, and E.J. Kostelich, Phys. Rev. E **67**, R035202 (2003).

[13] C. Grebogi, E. Kostelich, E. Ott, and J.A. Yorke, Physica D **25**, 347 (1987); F.J. Romeiras, C. Grebogi, E. Ott, and W.P. Dayawansa, *ibid.* **58**, 165 (1992).

[14] Y.-C. Lai, C. Grebogi, and J. Kurths, Phys. Rev. E **59**, 2907 (1999).

[15] R. Abraham and S. Smale, Proc. Symp. Pure Math. **14**, 5 (1970).

[16] Y.-C. Lai, M. Ding, and C. Grebogi, Phys. Rev. E **47**, 86 (1993).

[17] A. Katok and B. Hasselblatt, *Introduction to the Modern Theory of Dynamical System* (Cambridge University Press, Cambridge, England, 1995).

[18] G. Benettin, L. Galgani, A. Giorgilli, and J.-M. Strelcyn, Meccanica **15**, 21 (1980).

[19] Theoretical and numerical investigations on the characterization of the transition to high-dimensional chaos by unstable periodic orbits indicate that the transition is typically accompanied by severe unstable dimension variability [R.L. Davidchack and Y.-C. Lai, Phys. Lett. A **270**, 308 (2000)], which also leads to a smooth variation of the Lyapunov exponents (except the largest one) when they cross zero from the negative side [M.A. Harrison and Y.-C. Lai, Phys. Rev. E **59**, R3799 (1999)]. In fact, a quantitative measure for the degree of unstable dimension variability can be defined based on unstable periodic orbits, demonstrating that the variability is most severe at the transition [Y.-C. Lai, *ibid.* **59**, R3807 (1999)].

[20] Strictly, the random-walk model can be solved by the Fokker-Planck equation when Z is a zero-mean, Gaussian random variable. For our shadowing problem, numerically we find that the distribution of Z is approximately Gaussian (by definition Z has a zero mean).

[21] C.W. Gardiner, *Handbook of Stochastic Methods* (Springer-Verlag, New York, 1997); H. Risken, *The Fokker-Plank Equation* (Springer-Verlag, Berlin, 1989).

[22] It is useful to discuss our result in relation to the extended shadowing lemma in nonuniform hyperbolic systems. Suppose that the map $\mathbf{f}:\mathcal{R}^D \to \mathcal{R}^D$ is continuously differentiable and $\mathbf{\Sigma}$ is the invariant set of interest. Nonuniform hyperbolicity is a "weaker" type of hyperbolicity. In particular, for a diffeomorphism $\mathbf{g}:\mathcal{M} \to \mathcal{M}$ on a compact manifold $\mathcal{M}$, the invariant set $\mathbf{\Sigma}$ is *nonuniformly hyperbolic* if for every $\mathbf{x} \in \mathbf{\Sigma}$ the tangent space $\mathbf{T_x}$ can be split continuously, i.e., $\mathbf{T_x} = \mathbf{E_x^s} \oplus \mathbf{E_x^u}$ and, for sufficiently small $\epsilon > 0$ there is a *positive function* C_ϵ and $\lambda < 1 < \mu$ such that for every integer k, the following hold: (i) $C_\epsilon[\mathbf{g}^k(\mathbf{x})] \le e^{\epsilon|k|} C_\epsilon(\mathbf{x})$, (ii) $|\mathbf{D} \cdot \mathbf{g}^n(\mathbf{x}) \cdot \mathbf{y}| < C_\epsilon[\mathbf{g}^{m+k}(\mathbf{x})] \mu^n |\mathbf{y}|$ for $\mathbf{y} \in \mathbf{E_x^s}$, (iii) $|\mathbf{D} \cdot \mathbf{g}^{-n}(\mathbf{x}) \cdot \mathbf{y}| < C_\epsilon[\mathbf{g}^{m+k}(\mathbf{x})] \lambda^n |\mathbf{y}|$ for $\mathbf{y} \in \mathbf{E_x^u}$, and (iv) the angle between stable subspace and unstable subspace is bounded away from zero. The key feature associated with nonuniform hyperbolicity is that the positive number K for the definition of hyperbolicity is replaced by a positive function. The shadowing lemma in Ref. [17] guarantees the existence of long shadowing trajectories for nonuniformly hyperbolic dynamical systems. The nonhyperbolic systems studied here, i.e., dynamical systems with unstable-dimension variability, violate one of the essential conditions for hyperbolicity: the continuous splitting of the tangent space between the stable and unstable subspaces. Thus the shadowing lemma in Ref. [17] does not hold for these severely nonhyperbolic systems. For them, shadowing of numerical trajectories, even of relatively short lengths, cannot be expected. Our discovery of the combination of algebraic (for short time) and exponential (for long time) behaviors in the statistical distribution of the shadowing time answers the question "for how long

a numerical trajectory can be expected to be valid?" in a quantitative way.

[23] See, for example, J.F. Heagy, N. Platt, and S.M. Hammel, Phys. Rev. E **49**, 1140 (1994); D. Marthaler, D. Armbruster, Y.-C. Lai, and E.J. Kostelich, *ibid.* **64**, 016220 (2001).

[24] A. Čenys, A.N. Anagnostopoulos, and G.L. Bleris, Phys. Lett. A **224**, 346 (1997).

[25] This insight was first conceived by J.A. Yorke (private communication). The modeling problem was investigated in detail in the context of coupled chaotic oscillators in Ref. [10].

[26] While model solutions may not be valid for long time, the model may still be useful for yielding statistical or ergodic averages of physical quantities of interest [14]. An interesting question is how to identify situations in which models do not even yield useful statistical averages of physically relevant quantities [2,3].